CONSTRUCTING AND COMPRESSING GLOBAL MOMENT DESCRIPTORS FROM LOCAL ATOMIC ENVIRONMENTS

Vahe Gharakhanyan^{1*}, Max S. Aalto^{2,3}, Aminah Alsoulah³, Nongnuch Artrith⁴, Alexander Urban³

- ¹ Department of Applied Physics and Applied Mathematics, Columbia University, New York, NY, USA
- ² Physics and Informatics Laboratories, NTT Research, Inc., Sunnyvale, CA, USA
- ³ Department of Chemical Engineering, Columbia University, New York, NY, USA
- ⁴ Debye Institute for Nanomaterials Science, Utrecht University, Utrecht, Netherlands

ABSTRACT

Local atomic environment descriptors (LAEDs) are used in the materials science and chemistry communities, for example, for the development of machine learning interatomic potentials. Despite the fact that LAEDs have been extensively studied and benchmarked for various applications, global structure descriptors (GSDs), i.e., descriptors for entire molecules or crystal structures, have been mostly developed independently based on other approaches. Here, we propose a systematically improvable methodology for constructing a space of representations of GSDs from LAEDs by incorporating statistical information and information about chemical elements. We apply the method to construct GSDs of varying complexity for lithium thiophosphate structures that are of interest as solid electrolytes and use an information-theoretic approach to obtain an optimally compressed GSD. Finally, we report the performance of the compressed GSD for energy prediction tasks.

1 Introduction

Local atomic environment descriptors (LAEDs) are widely used in the materials science and chemistry communities, for example, in machine learning interatomic potentials (force fields) and for detecting (dis)similarities between atomic environments (Parsaeifard et al., 2021; Langer et al., 2022). An early example is the atom-centered *symmetry functions* introduced by Behler and Parrinello (Behler & Parrinello) (2007; Behler) (2011) to describe the chemical environment of atoms as input to atomic neural networks. Since then, various other LAED methods have been proposed in the literature and broadly applied to research questions in chemistry and materials science (Drautz, 2019; Onat et al., 2020; Musil et al., 2021; Langer et al., 2022). In parallel, global structure descriptors (GSDs) for entire molecules and crystal structures have independently been developed, though, for periodic crystal structures, only a few representations have been proposed (Damewood et al., 2023). So far, less emphasis has been placed on constructing GSDs from LAEDs for learning tasks where the property of interest cannot be intuitively decomposed into atomic contributions, for example, for predicting elastic properties such as the bulk modulus. Given that LAEDs have been extensively benchmarked, it would be desirable to leverage this experience for the construction of GSDs as well.

Prior work includes examples of constructing GSDs by evaluating the mean of the LAEDs for a given atomic structure (Priedeman et al., 2018; Cheng et al., 2020). Other authors proposed to include the variance in addition to the mean to combine all LAEDs of sites with the same chemical element (Guo et al., 2022). Higher mathematical moments have been used to construct invertible LAEDs with prospective applications for materials discovery through inverse design tasks (Uhrin, 2021). Here, we build on and extend these ideas to formalize the construction of GSDs by combining chemical information and structural statistics via a moment expansion of the distribution of atomic environment descriptors. We then use a recently introduced information-theoretic approach (Glielmo et al., 2022; Darby et al., 2022a; b) to inspect the relationship of the GSD information

^{*}Correspondence to vg2471@columbia.edu and au2229@columbia.edu

content with its complexity and determine the GSDs that offer the optimal compromise between the information content about the atomic system and the descriptor complexity (Zeni et al., 2021). Khan et al., 2023). Finally, we demonstrate the performance of our proposed descriptors for energy prediction tasks.

2 METHODOLOGY

We adopt the following notation. The structure data set \mathbb{S} consists of atomic structures s that in turn contain the sites $\{a_1,...,a_{n_1},b_1,...,b_{n_2},...\}$ with corresponding element types $\{A,B,...\}$. The LAED of site a in structure s is denoted $\sigma_a^{(s)}$ and is a real-valued vector. Note that the present work is independent of the method that is used to obtain $\sigma_a^{(s)}$.

2.1 Chemical Element descriptor

We call *chemical element descriptor* (CED) a representation of all sites of the same chemical element in a given structure. A CED can be constructed by combining the information of the LAEDs of all sites of a given element type. Simply averaging all LAEDs would potentially result in a significant loss of information. One way to systematically go beyond the mean LAED is by taking into account the statistics through mathematical moments. The first moment of a distribution is the mean, and general moments of order two (variance) and above are given by $\mu_n(\mathbb{X}) = \frac{1}{N} \sum_{i=1}^N \left(X_i - \bar{X}\right)^n$. The mean of the LAEDs thus corresponds to a CED with an inner-moment degree of $1 \ (n_{\rm in} = 1)$. To incorporate higher moments in the CED, we can stack (concatenate) different moment descriptors: $\sigma_A^{(s)} = \bigoplus_{i=0}^{n_{\rm in}} \mu_i(\{\sigma_a^{(s)} \mid \forall a \in A, \ A \in s\})$, where the \bigoplus operator concatenates its arguments into a single CED vector with dimensions of $d^{(A)} = d^{(a)} \cdot n_{\rm in}$, where $d^{(a)}$ is the dimension of the LAED.

2.2 Global structure descriptor

We propose different methods for obtaining a *global structure descriptor* (GSD) from LAEDs and CEDs. A global structure descriptor can be constructed from:

- i: LAEDs, by finding the moments up to a degree of outer-moment (n_{out}) of the distribution of all (element-weighted) LAEDs,
- ii: CEDs, by stacking CEDs for all chemical elements,
- iii: CEDs, by finding the moments up to a degree of outer-moment of the distribution of (element-weighted) CEDs.

$$\sigma^{(s)} = \begin{cases} \text{i:} & \bigoplus_{i=0}^{n_{\text{out}}} \mu_i(\{w_A \cdot \sigma_a^{(s)} \mid a \in A, \ \forall a \in s\}), & \text{if } n_{\text{out}} \in \{1, 2, ...\} \text{ and } n_{\text{in}} = 0. \\ \text{ii:} & \bigoplus_{A \in s} \sigma_A^{(s)}, & \text{if } n_{\text{out}} = 0 \text{ and } n_{\text{in}} \in \{1, 2, ...\}. \\ \text{iii:} & \bigoplus_{i=0}^{n_{\text{out}}} \mu_i(\{w_A \cdot \sigma_A^{(s)} \mid \forall A \in s\}), & \text{if } n_{\text{out}}, n_{\text{in}} \in \{1, 2, ...\}. \end{cases}$$

$$(1)$$

The element weighting can be turned off by setting w=1 for all elements. Note that the LAEDs themselves can already incorporate chemical information, for example, through element weightings (Artrith et al., 2017). The dimension of the final global structure descriptor is $d^{(s)}=d^{(a)}\cdot\max(1,n_{\text{out}})\cdot\max(1,n_{\text{in}})$ for methods i and iii, and, for method ii, is additionally scaled by the number of unique elements in $\mathbb S$. For multi-element data sets, where not all structures contain all element types, GSD from method ii should be correctly zero-padded to achieve consistent GSD dimensions among all structures. Besides the three GSD construction methods shown above, we can create new GSDs by simply stacking different GSD constructions discussed (i.e., stacking GSDs from methods iii and i, or descriptors from method i or iii with and without element weightings).

¹Here, "inner" refers to the CED construction and "outer" to the GSD construction of section 2.2

2.3 Information content and compression

The number of inner and outer moments considered, as well as the number of unique elements in the data set, can increase the GSD dimension. We define the complexity of a descriptor as $d^{(s)}/d^{(a)}$. It is important to quantify the information that each new moment adds about the system and to create methods for determining the best dimension/construction method of the GSD that contains the necessary structural and chemical information. In other words, we're looking for the optimum combination of inner and outer moments and element weightings that can be obtained by compressing the full GSD with minimal loss of information.

To compress the descriptor, we need to quantify the information content (or loss) between compressed and full descriptors. We can choose between information content measures based on distances or ranks, the latter being preferred because it is agnostic to the scaling of the space. Here, we use an information imbalance between two descriptors based on ranks (also called rank information imbalance - RIM), recently introduced by Glielmo et al. (2022): $\Delta R(\Sigma_1 \to \Sigma_2) =$ $\frac{1}{N} \sum_{\mathbf{s_i}, \mathbf{s_j} \in \mathbb{S}} \left(r_{s_i s_j}^{(\Sigma_2)} \mid r_{s_i s_j}^{(\Sigma_1)} = 1 \right), \text{ where } r_{s_i s_j}^{(\Sigma)} \text{ is the rank between GSDs of structures } s_i \text{ and } s_j \text{ in } s_i = 1$ descriptor space Σ . The rank $r_{s_i s_i}$ is computed by sorting the distances between GSD of s_i and all other structure descriptors from smallest to largest and then finding the corresponding index for s_i . So, for instance, a rank of 1 means that GSDs of s_i and s_i are nearest neighbors in the given descriptor space. To find the rankings, we use Euclidean distance as the distance metric. So rank information imbalance computes the average rank in descriptor space Σ_2 for the structures that are nearest neighbors in descriptor space Σ_1 . If $\Delta R(\Sigma_1 \to \Sigma_2) \approx 1$, then descriptor Σ_1 is informative of descriptor Σ_2 . The higher the imbalance, the less informative Σ_1 becomes for Σ_2 . It is important to note here that the rank imbalance is not symmetric $(\Delta R(\Sigma_1 \to \Sigma_2) \neq \Delta R(\Sigma_2 \to \Sigma_1))$ because the sets of pairs of nearest neighbors in different descriptor spaces are, almost often, different. For this reason, similar to Glielmo et al. (2022), we can construct a symmetric full rank information imbalance (SRIM) as follows: $\Delta \bar{R}(\Sigma_1, \Sigma_2) = \frac{1}{2} [\Delta R(\Sigma_1 \to \Sigma_2) + \Delta R(\Sigma_2 \to \Sigma_1)].$ Both information imbalance measures discussed have a lower limit of 1, meaning that both spaces are equivalent (all nearest-neighbor pairs in both descriptor spaces are the same), and the upper limit will depend on the number of structures in the data set.

3 Results and discussion

3.1 CONSTRUCTION OF GLOBAL STRUCTURE DESCRIPTORS

Data set: We used 6055 previously published computationally generated atomic structures of glass-ceramic lithium thiophosphates (LPS) with compositions on or close to the composition line $(\text{Li}_2\text{S})_x(\text{P}_2\text{S}_5)_{1-x}$ (Guo et al., [2022]).

Local atomic environment descriptor: We employed a LAED based on the truncated Chebyshev expansions of the radial and angular distribution functions (RDF and ADF) (Artrith et al., 2017). This LAED method is numerically efficient and has the advantage that its dimension does not increase with the number of chemical elements; it is also invariant with respect to rotations, translations, and atom permutations (Artrith & Urban, 2016). For all elements, we used a cutoff of 6.0 Å with expansion order 19 for the RDF and a cutoff of 3.0 Å with expansion order 5 for the ADF. The LAED is a stacking of four sets of expansion coefficients: the coefficients of the RDF and ADF with and without element weightings, leading to a total LAED dimension of $2 \times (19 + 5) = 48$ (Guo et al., 2022). The following element weightings were used: Li: -1, P: 0, and S: +1.

Global structure descriptor: GSDs with all possible combinations of outer and inner moments up to a degree of five, with and without element weightings (using the LAED weightings), were constructed. In the following, Σ_{ijk} denotes a GSD with outer moments up to a degree of i, inner moments up to a degree of j, and with (k=1) or without (k=0) element weightings. For example, Σ_{231} and Σ_{230} represent GSDs with and without element weighting, respectively, that are constructed with outer moments of up to a degree of two (average and variance) and inner moments of up to a degree of three (average, variance, and third moment). Note that GSDs of type Σ_{0j1} do not exist, according to equation Π . Element-weighted and unweighted GSDs with $i \neq 0$ and identical

inner (i) and outer (j) moments can be combined via concatenation to create new GSDs, Σ_{ij2} ; for example, $\Sigma_{232} = \Sigma_{230} \oplus \Sigma_{231}$. With such concatenation, we further construct two GSDs that contain the most information about the geometry statistics and chemistry, $\Sigma_{555} = \Sigma_{552} \oplus \Sigma_{502} \oplus \Sigma_{050}$ and $\Sigma_{554} = \Sigma_{552} \oplus \Sigma_{502}$. Σ_{555} and Σ_{554} have the dimensions 3600 and 2880, and complexities 75 and 60, respectively. Enumerating all distinct combinations of GSDs with moments up to order 5 and their concatenations resulted in a GSD space with 97 distinct representations. All descriptors were normalized to remove the scale imbalance from using higher-order moments.

3.2 Complexity analysis

By design, most of the constructed GSDs are contained within other GSDs, and most information is contained in Σ_{555} , followed by Σ_{554} . Here, we aim to identify those lower-dimensional descriptors that exhibit minimal information loss compared to these two references. For this purpose, we evaluated the RIMs between all $97 \times 96 = 9312$ pairs of GSDs.

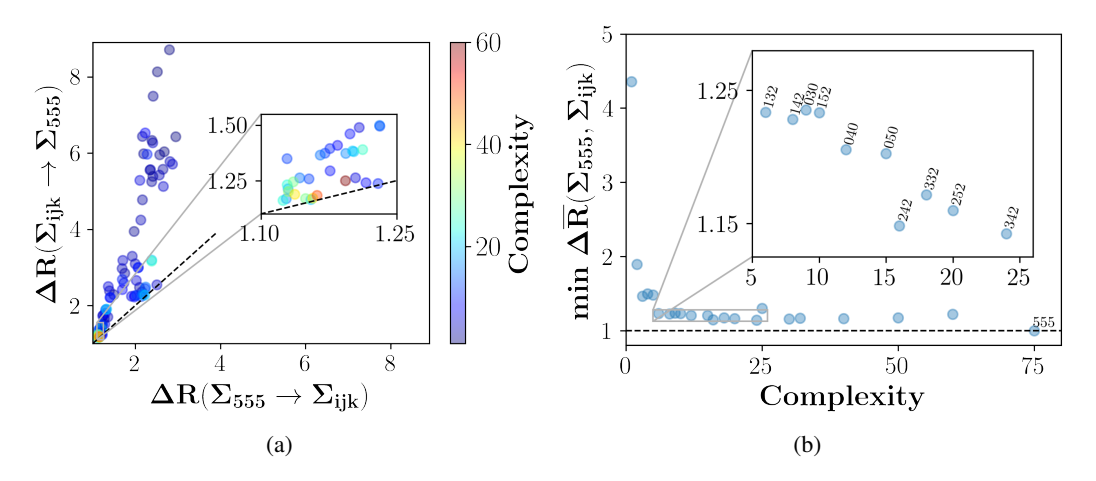


Figure 1: (a) Correlation plot between rank information imbalances of inferring all other descriptors from Σ_{555} (on x-axis) and inferring Σ_{555} from all other descriptors (on y-axis). (b) Minimum symmetric rank information imbalance between Σ_{555} and all other descriptors as a function of the descriptor complexity.

Figure Π_b shows a correlation plot between the RIMs for inferring each descriptor space from Σ_{555} and inferring Σ_{555} from each descriptor space. GSDs with high complexity (> 30) exhibit minor information loss (i.e., retain most information content) when inferring Σ_{555} from them or inferring them from Σ_{555} . Figure Π_b shows the minimum SRIM between Σ_{555} and other descriptors for a given complexity value. We observe that increasing the complexity beyond Σ_{242} does not affect the SRIM substantially. By comparing the results with Figure B.1b that shows a similar SRIM analysis for Σ_{554} , it is apparent that $\Sigma_{i,j,k=2}$ descriptors have the most information content and least information loss for both Σ_{554} and $\widetilde{\Sigma}_{555}$. Here we did not mention descriptors $\Sigma_{0,j>2,0}$ because, although their performance towards Σ_{555} is good, they provide a worse interpretation for Σ_{554} , and the reason most likely is that Σ_{554} does not contain Σ_{050} . The raw data is given in Table B.2 and exhibits the same trend: $\Sigma_{i,j,k=2}$ descriptors are most informative about the other GSDs (see also Table B.1) and can be inferred best from other descriptors (Table B.3). This means incorporating only structural/geometric information (with Σ_{ij0} -type descriptors) is insufficient, and the addition of chemical information to the descriptor through element weightings adds the missing information content. Table B.I also shows that simple averaging of all LAEDs with or without element weighting (Σ_{101} and $\overline{\Sigma}_{100}$, respectively) has the worst overall performance. Such descriptors might be useful if all atomic environments are similar in composition, but if the environments vary drastically (Figure A.1), simple averaging and disregarding chemical information leads to information loss. While Σ_{101} and Σ_{100} are the worst for inferring other GSDs, the data in Table B.3 shows that it is the hardest to infer Σ_{050} from other GSDs. This is intuitive because $\Sigma_{i>0,j,k\in\{0,1\}}$ GSDs lose either the distinct elemental information by including only element-weight agnostic moments or lose the distinct geometry information by including element-weighted moments. From Table B.4, we see that GSDs that are most similar to each other contain higher moments and the same method for the descriptor construction. This exemplifies that adding the next higher moment to the descriptor results in a decreasing information gain, i.e., the GSDs converge with the order of the moment expansion. From Table B.5, the most dissimilar descriptors are those constructed with different methods, meaning that different construction methods will result in including different pieces of information.

3.3 Energy fittings

In the previous section, we assessed the information content in different GSDs. Here, we investigate whether high information content is indeed beneficial for learning tasks. We trained on a subset of formation energies of those structures in the LPS dataset that are exactly on the $(\text{Li}_2S)_x(P_2S_5)_{1-x}$ composition line (Guo et al., 2022). We used a gradient-boosted tree model with four different numbers of estimators to accommodate the varying complexity of GSDs. Training and test set splits of 9 to 1 over five random seed numbers were used (Figure C.1). From the mean absolute error (MAE) and root mean squared error (RMSE) plots, it can be seen that indeed Σ_{100} and Σ_{101} are performing the worst towards the energy training task. $\Sigma_{i,j,k=2}$ descriptors perform better, although they do not reach the accuracy of the full Σ_{555} descriptor. Interestingly, the descriptor that, on average, contained most information about other descriptors (Table B.2), Σ_{332} , is performing second best after the full descriptor and performs equivalently when considering the MAE only. Overall, the scale of energy errors is on the same order of magnitude as the state-of-the-art neural network interatomic potentials, even though the tree models and LAED parameters were not optimized. Important to observe that the relative rankings of optimal GSDs from the information-theoretic approach and energy models are slightly different. One reason is that the models were trained on a subset of LPS structures (about 2/3 of the original data set) and evaluated on a test set that contains only 7% of all structures. To conclude, the results of the information-theoretic approach and energy models are sensitive to the data set used. A similar analysis should first be performed for a new data set before choosing an optimally compressed descriptor. See Appendix D and E for further discussion. This analysis leads to two conclusions: (i) it is apparent that the complexity of the full descriptor is not needed, and models with similar or equivalent performance can be obtained with less complex GSDs, (ii) the systematic convergence of the GSDs seen in the information imbalance is also reflected by the performance of the energy models.

4 Conclusion

We introduced a systematic framework for constructing computationally efficient and property-independent global structure descriptors from local atomic environment descriptors by incorporating both geometry statistics through mathematical moments and chemistry through element weightings. We demonstrated for a set of glassy/amorphous lithium thiophosphate structures how global descriptors with an optimal balance of information content and complexity can be identified, and we confirmed the descriptor performance with an energy prediction task. In future work, we plan to investigate how the hyperparameters of the local atomic environment descriptor affect the performance of the global descriptor, how the descriptors perform for different moment expansions (through standardized moments or cumulants) and on much larger materials data sets with diverse chemical elements.

CODE AVAILABILITY

The code to construct global structure descriptors from local environment descriptors is implemented in menet software package and can be found in https://github.com/atomisticnet/aenet-python open source repository.

ACKNOWLEDGEMENTS

This work was supported by the National Science Foundation under Grant No. DMR-1940290 (Harnessing the Data Revolution, HDR). The authors thank Dallas R. Trinkle and Snigdhansu Chatterjee for helpful discussions.

REFERENCES

- Nongnuch Artrith and Alexander Urban. An implementation of artificial neural-network potentials for atomistic materials simulations: Performance for tio2. *Computational Materials Science*, 114: 135–150, 2016.
- Nongnuch Artrith, Alexander Urban, and Gerbrand Ceder. Efficient and accurate machine-learning interpolation of atomic energies in compositions with many species. *Physical Review B*, 96(1): 014112, 2017.
- Jörg Behler. Atom-centered symmetry functions for constructing high-dimensional neural network potentials. *The Journal of chemical physics*, 134(7):074106, 2011.
- Jörg Behler and Michele Parrinello. Generalized neural-network representation of high-dimensional potential-energy surfaces. *Physical review letters*, 98(14):146401, 2007.
- Bingqing Cheng, Ryan-Rhys Griffiths, Simon Wengert, Christian Kunkel, Tamas Stenczel, Bonan Zhu, Volker L Deringer, Noam Bernstein, Johannes T Margraf, Karsten Reuter, et al. Mapping materials and molecules. Accounts of Chemical Research, 53(9):1981–1991, 2020.
- James Damewood, Jessica Karaguesian, Jaclyn R Lunger, Aik Rui Tan, Mingrou Xie, Jiayu Peng, and Rafael Gómez-Bombarelli. Representations of materials for machine learning. arXiv preprint arXiv:2301.08813, 2023.
- James P Darby, James R Kermode, and Gábor Csányi. Compressing local atomic neighbourhood descriptors. *npj Computational Materials*, 8(1):166, 2022a.
- James P Darby, Dávid P Kovács, Ilyes Batatia, Miguel A Caro, Gus LW Hart, Christoph Ortner, and Gábor Csányi. Tensor-reduced atomic density representations. arXiv preprint arXiv:2210.01705, 2022b.
- Ralf Drautz. Atomic cluster expansion for accurate and transferable interatomic potentials. *Physical Review B*, 99(1):014104, 2019.
- Aldo Glielmo, Claudio Zeni, Bingqing Cheng, Gábor Csányi, and Alessandro Laio. Ranking the information content of distance measures. *PNAS Nexus*, 1(2):pgac039, 2022.
- Haoyue Guo, Qian Wang, Alexander Urban, and Nongnuch Artrith. Artificial intelligence-aided mapping of the structure–composition–conductivity relationships of glass–ceramic lithium thiophosphate electrolytes. *Chemistry of Materials*, 34(15):6702–6712, 2022.
- Danish Khan, Stefan Heinen, and O Anatole von Lilienfeld. Quantum machine learning at record speed: Many-body distribution functionals as compact representations. *arXiv* preprint *arXiv*:2303.16312, 2023.
- Marcel F Langer, Alex Goeßmann, and Matthias Rupp. Representations of molecules and materials for interpolation of quantum-mechanical simulations via machine learning. *npj Computational Materials*, 8(1):41, 2022.
- Felix Musil, Andrea Grisafi, Albert P Bartók, Christoph Ortner, Gábor Csányi, and Michele Ceriotti. Physics-inspired structural representations for molecules and materials. *Chemical Reviews*, 121 (16):9759–9815, 2021.
- Berk Onat, Christoph Ortner, and James R Kermode. Sensitivity and dimensionality of atomic environment representations used for machine learning interatomic potentials. *The Journal of Chemical Physics*, 153(14):144106, 2020.
- Behnam Parsaeifard, Deb Sankar De, Anders S Christensen, Felix A Faber, Emir Kocer, Sandip De, Jörg Behler, O Anatole von Lilienfeld, and Stefan Goedecker. An assessment of the structural resolution of various fingerprints commonly used in machine learning. *Machine Learning: Science and Technology*, 2(1):015018, 2021.
- Jonathan L Priedeman, Conrad W Rosenbrock, Oliver K Johnson, and Eric R Homer. Quantifying and connecting atomic and crystallographic grain boundary structure using local environment representation and dimensionality reduction techniques. *Acta Materialia*, 161:431–443, 2018.

Martin Uhrin. Through the eyes of a descriptor: constructing complete, invertible descriptions of atomic environments. *Physical Review B*, 104(14):144110, 2021.

Claudio Zeni, Kevin Rossi, Aldo Glielmo, and Stefano De Gironcoli. Compact atomic descriptors enable accurate predictions via linear models. *The Journal of Chemical Physics*, 154(22):224112, 2021.

A APPENDIX: STATISTICS OF INDIVIDUAL COMPONENTS OF THE FULL GLOBAL STRUCTURE DESCRIPTOR

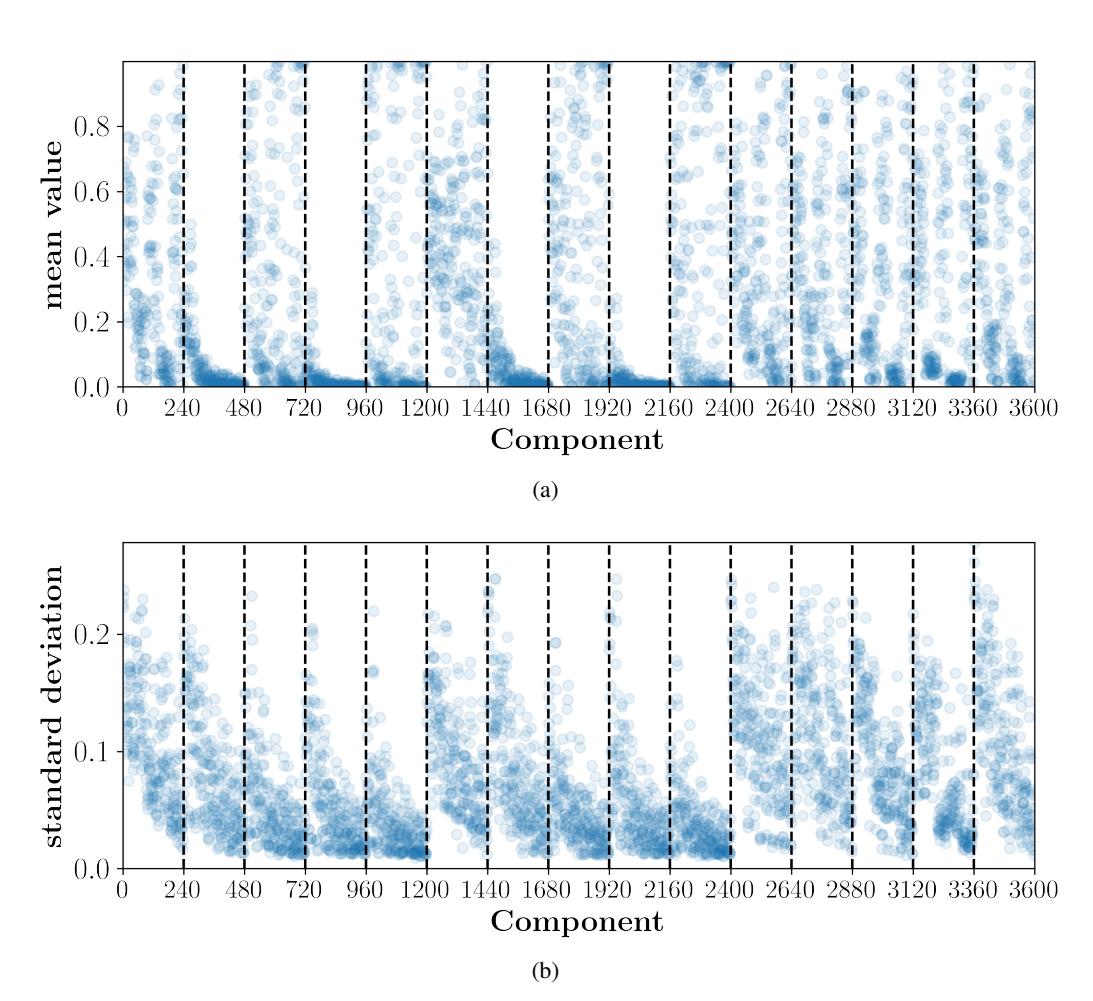


Figure A.1: (a) Mean and (b) standard deviation values of each component in Σ_{555} global structure descriptor.

B APPENDIX: ADDITIONAL INFORMATION IMBALANCE ANALYSIS

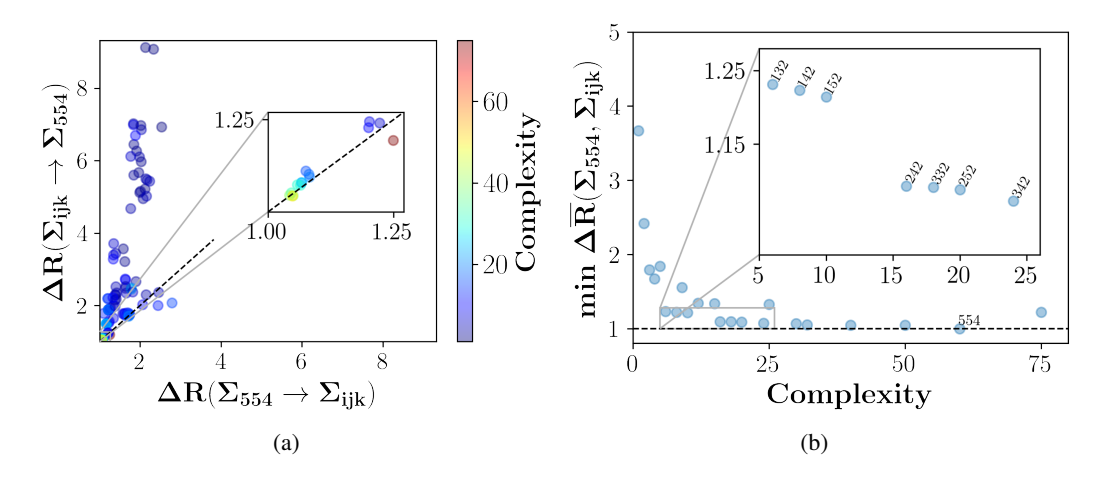


Figure B.1: (a) Correlation plot between rank information imbalances of inferring all other descriptors from Σ_{554} (on x-axis) and inferring Σ_{554} from all other descriptors (on y-axis). (b) Minimum symmetric rank information imbalance between Σ_{554} and all other descriptors as a function of the descriptor complexity.

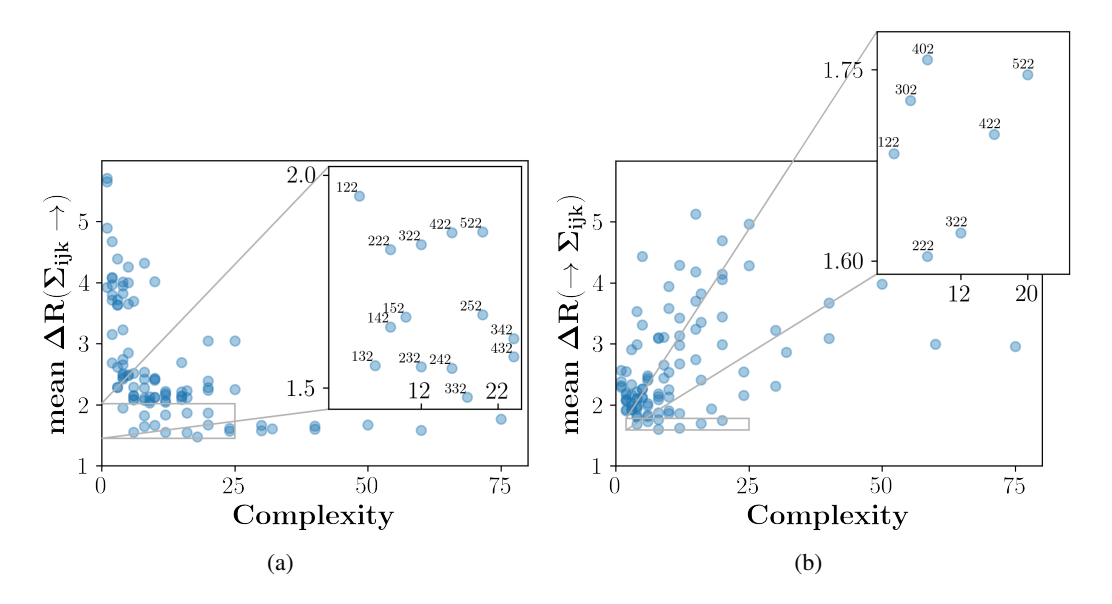


Figure B.2: (a) Mean rank information imbalance of inferring all other descriptors from the given descriptor with the given complexity. (b) Mean information imbalance of inferring the given descriptor with the given complexity from all other descriptors.

Table B.1: Global descriptors sorted by the average of symmetric rank information imbalance $\left(\left\langle \Delta\bar{R}\right\rangle \right).$

Σ_1	$\langle \Delta R_{1\to 2} \rangle$	$\langle \Delta R_{2\to 1} \rangle$	$\langle \Delta ar{R} angle$
132	1.553	1.807	1.680
232	1.550	1.862	1.706
332	1.478	1.938	1.708
222	1.825	1.604	1.714
322	1.837	1.622	1.730
422	1.864	1.699	1.782
522	1.867	367 1.746	
122	1.950	1.684	1.817
432	1.573	2.158	1.865
302	2.083	1.726	1.904
142	1.643	2.182	1.913
402	2.077	1.758	1.918
532	1.577 2.310	2.310	1.944
242	1.546	2.411	1.978
502	2.126	1.858	1.992
010	4.389	1.928	3.159
040	2.045	4.291	3.168
251	2.402	3.940	3.171
510	4.255	2.109	3.182
541	2.282	4.147	3.214
550	2.249	4.283	3.266
102	4.671	2.172	3.421
351	2.693	4.183	3.438
050	2.136	5.127	3.631
151	2.852	4.433	3.643
110	4.891	2.564	3.728
451	3.049	4.691	3.870
551	3.043	4.961	4.002
100	5.710	2.314	4.012
101	5.651	2.384	4.017

Table B.2: Global descriptors sorted by the average of information they contain about all other descriptors $(\langle \Delta R_{1 \to 2} \rangle)$.

-	/ A . D . \	/ A . D . \	/ A = 5\
Σ_1	$\langle \Delta R_{1\rightarrow 2} \rangle$	$\langle \Delta R_{2\rightarrow 1} \rangle$	$\langle \Delta R \rangle$
332	1.478	1.938	1.708
242	1.546	2.411	1.978
232	1.550	1.862	1.706
132	1.553	1.807	1.680
432	1.573	2.158	1.865
532	1.577	2.310	1.944
554	1.586	2.998	2.292
542	1.604	3.088	2.346
442	1.605	2.861	2.233
342	1.616	2.540	2.078
142	1.643	2.182	1.913
452	1.651	3.670	2.660
352	1.662	3.226	2.444
152	1.666	2.538	2.102
252	1.672	2.986	2.329
•••	•••	•••	•••
111	3.923	2.291	3.107
410	3.949	2.097	3.023
210	3.965	2.070	3.018
511	3.998	2.258	3.128
411	4.011	2.212	3.112
512	4.015	1.906	2.961
112	4.075	1.924	2.999
201	4.089	2.073	3.081
510	4.255	2.109	3.182
412	4.317	1.875	3.096
010	4.389	1.928	3.159
102	4.671	2.172	3.421
110	4.891	2.564	3.728
101	5.651	2.384	4.017
100	00 5.710 2.314	4.012	

Table B.3: Global descriptors sorted by the average of information all other descriptors contain about them $(\langle \Delta R_{1 \to 2} \rangle)$.

	Σ_2	$\langle \Delta R_{1\to 2} \rangle$	$\langle \Delta R_{2\to 1} \rangle$	$\langle \Delta ar{R} angle$
-	222	1.604	1.825	1.714
	322	1.622	1.837	1.730
	122	1.684	1.950	1.817
	422	1.699	1.864	1.782
	302	1.726	2.083	1.904
	522	1.746	1.867	1.806
	402	1.758	2.077	1.918
	202	1.800	2.742	2.271
	132	1.807	1.553	1.680
	212	1.824	3.227	2.526
	312	1.833	3.694	2.764
	502	1.858	2.126	1.992
	232	1.862	1.550	1.706
	412	1.875	4.317	3.096
	200	1.905	3.155	2.530
	250	3.583	2.120	2.851
	452	3.670	1.651	2.660
	350	3.703	2.085	2.894
	441	3.821	2.231	3.026
	251	3.940	2.402	3.171
	552	3.979	1.674	2.827
	450	4.057	2.239	3.148
	541	4.147	2.282	3.214
	351	4.183	2.693	3.438
	550	4.283	2.249	3.266
	040	4.291	2.045	3.168
	151	4.433	2.852	3.643
	451	4.691	3.049	3.870
	551	4.961	3.043	4.002
	050	5.127	2.136	3.631

Table B.4: Most similar pairs of descriptors according to the symmetric rank information imbalance $(\Delta \bar{R})$. Note that not all decimal points are shown here.

Σ_1	Σ_2	$\Delta R_{1\to 2}$	$\Delta R_{2\rightarrow 1}$	$\Delta ar{R}$
450	550	1.010	1.009	1.010
420	520	1.011	1.011	1.011
421	521	1.011	1.011	1.011
440	540	1.012	1.011	1.011
442	542	1.012	1.011	1.011
411	511	1.012	1.012	1.012
432	532	1.012	1.011	1.012
451	551	1.013	1.012	1.012
422	522	1.012	1.012	1.012
431	531	1.012	1.013	1.012
452	552	1.013	1.012	1.012
430	530	1.014	1.012	1.013
412	512	1.014	1.013	1.013
441	541	1.015	1.013	1.014
401	501	1.017	1.017	1.017
340	440	1.018	1.018	1.018
311	411	1.020	1.019	1.019
410	510	1.022	1.019	1.020
352	452	1.021	1.020	1.020
330	430	1.022	1.020	1.021
252	352	1.021	1.021	1.021
341	441	1.025	1.019	1.022
320	420	1.023	1.021	1.022
340	350	1.023	1.021	1.022
342	442	1.020	1.025	1.022
232	332	1.024	1.021	1.023
351	451	1.023	1.022	1.023
140	150	1.024	1.021	1.023
251	351	1.023	1.022	1.023
322	422	1.023	1.023	1.023
•••	•••			

Table B.5: Most dissimilar pairs of descriptors according to the symmetric rank information imbalance $(\Delta \bar{R})$.

Σ_1	Σ_2	$\Delta R_{1\to 2}$	$\Delta R_{2\rightarrow 1}$	$\Delta \bar{R}$
	•••			
452	101	2.467	11.708	7.088
441	100	2.310	11.897	7.104
452	100	2.590	11.701	7.145
112	551	11.392	2.961	7.176
251	101	2.562	11.889	7.225
450	101	3.987	10.571	7.279
102	451	11.475	3.088	7.282
550	100	3.669	10.898	7.283
102	050	11.772	2.956	7.364
151	101	3.195	11.574	7.384
552	100	2.581	12.383	7.482
541	101	2.237	12.750	7.493
541	100	2.305	12.729	7.517
102	551	12.050	3.044	7.547
550	101	4.002	11.094	7.548
552	101	2.445	12.721	7.583
110	351	10.666	4.502	7.584
111	050	11.867	3.381	7.624
100	050	12.164	3.132	7.648
251	100	2.720	12.647	7.683
151	100	3.413	12.272	7.843
101	050	12.383	3.340	7.862
351	101	2.902	13.145	8.023
110	451	12.108	4.468	8.288
351	100	3.442	13.150	8.296
110	551	12.544	4.392	8.468
451	101	2.978	14.054	8.516
551	101	2.925	15.045	8.985
451	100	3.518	14.626	9.072
551	100	3.469	15.415	9.442

C APPENDIX: A GRADIENT-BOOSTED TREE MODEL FOR FORMATION ENERGY PREDICTIONS

We used a gradient-boosted tree model to determine if our results can compare to those from the state-of-the-art neural network interatomic potential models.

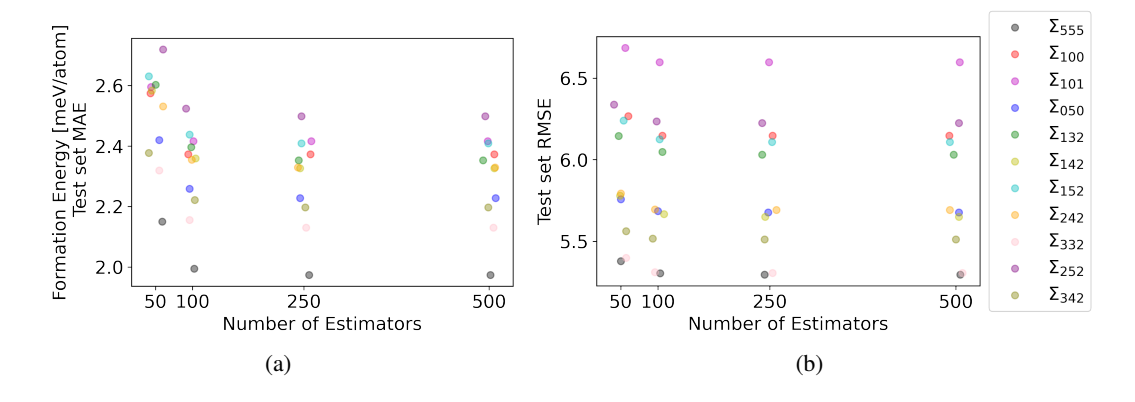


Figure C.1: Average (a) MAE and (b) RMSE scores for the test set of formation energy training on a subset of the LPS dataset. A horizontal jitter is applied to the points to help differentiate global structure descriptors.

D APPENDIX: COMPARISON BETWEEN THE WHOLE AND LIMITED DATA SETS

In the main body of the paper, we have performed the energy fittings on a smaller data set of structures (compared to the dataset used for the information-theoretic analysis). Here, we compare the results from the information-theoretic study on the whole and limited data sets. From Figures [D.1], [D.2] and [D.3], the choice of the data set (in our case slightly) affects the relative ranking of optimally compressed descriptors. For this reason, a similar analysis should first be performed for a new data set before choosing an optimally compressed descriptor.

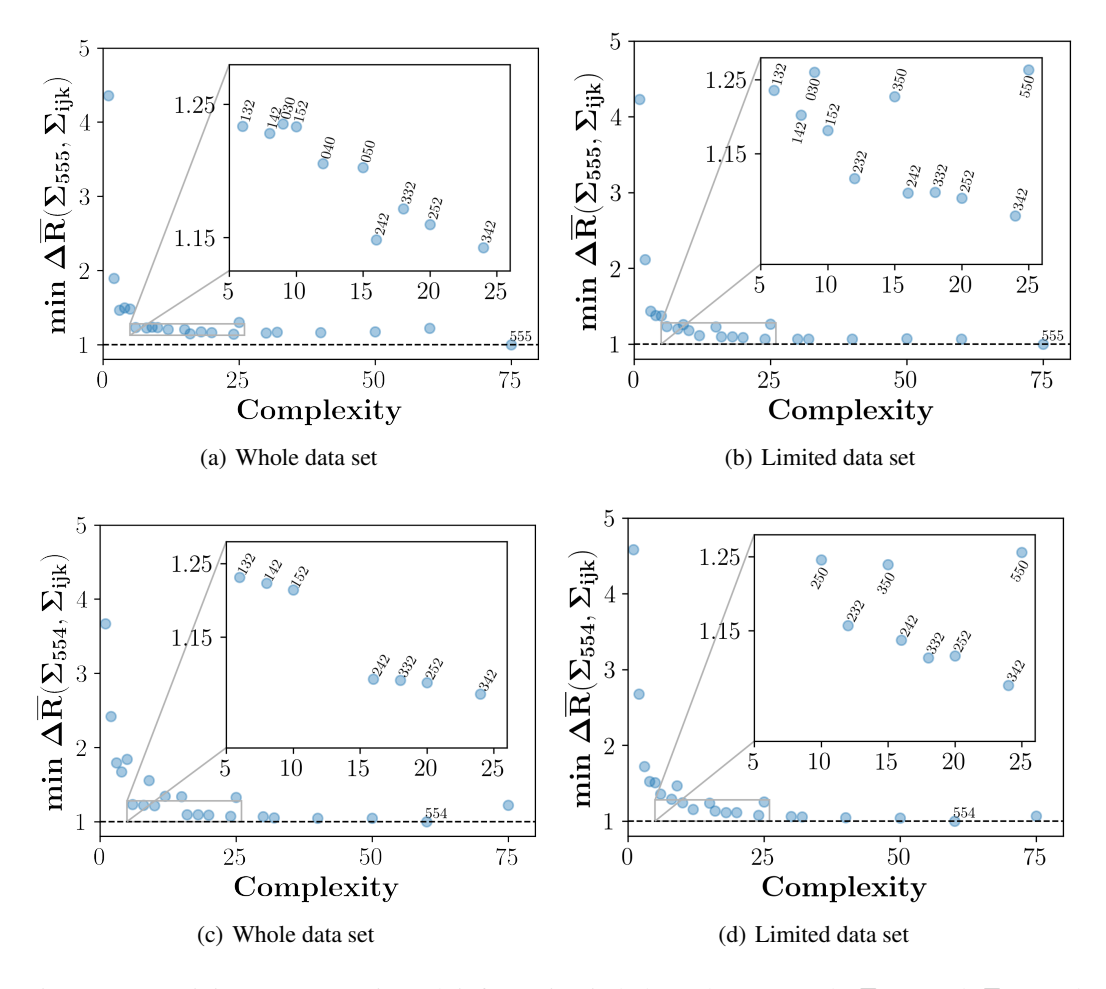


Figure D.1: Minimum symmetric rank information imbalance between (a,b) Σ_{555} , (c,d) Σ_{554} and all other descriptors as a function of the descriptor complexity for (a,c) the whole and (b,d) limited data sets.

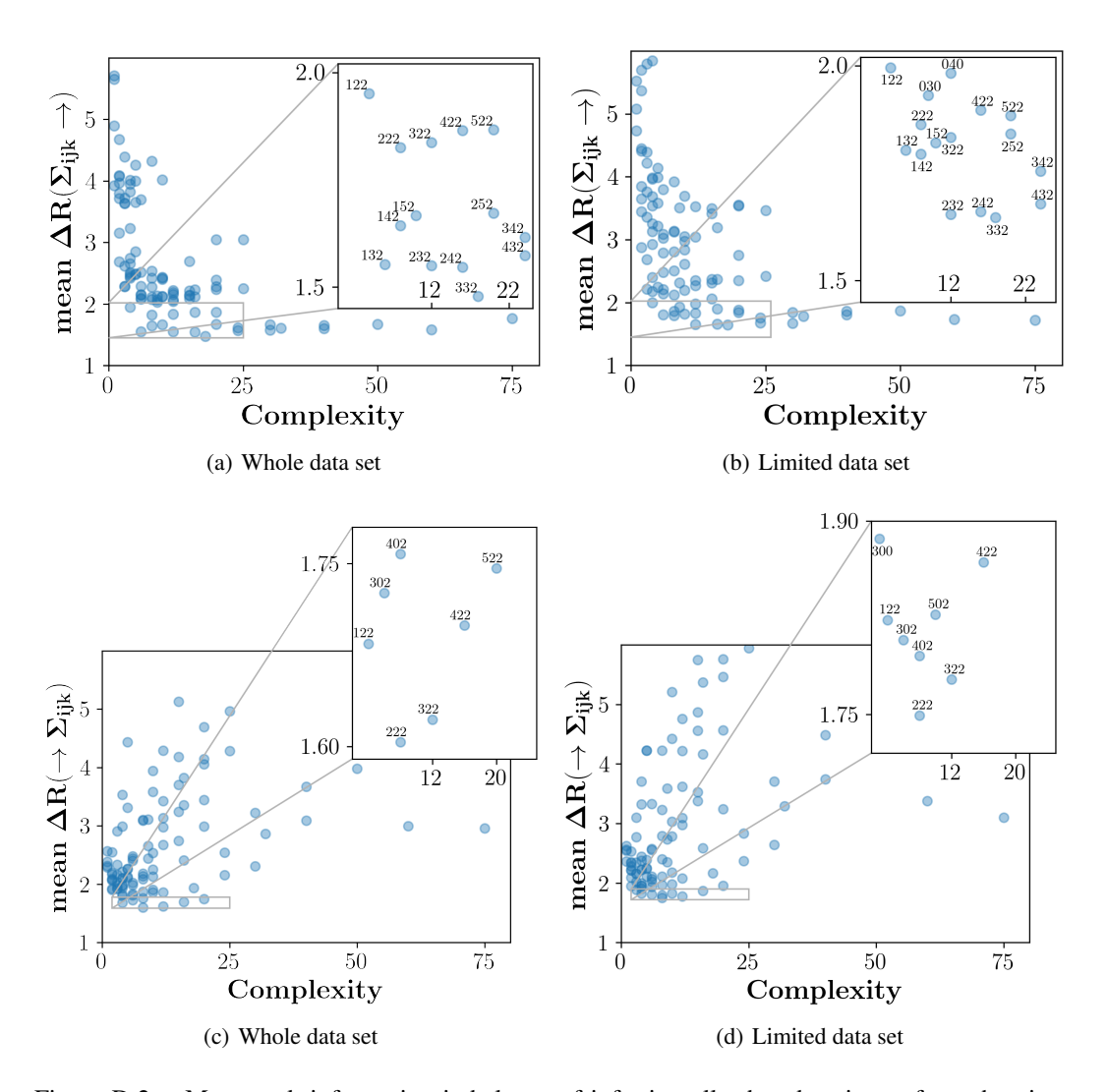


Figure D.2: Mean rank information imbalance of inferring all other descriptors from the given descriptor with the given complexity for (a) the whole and (b) limited data sets. Mean information imbalance of inferring the given descriptor with the given complexity from all other descriptors for (c) the whole and (d) limited data sets.

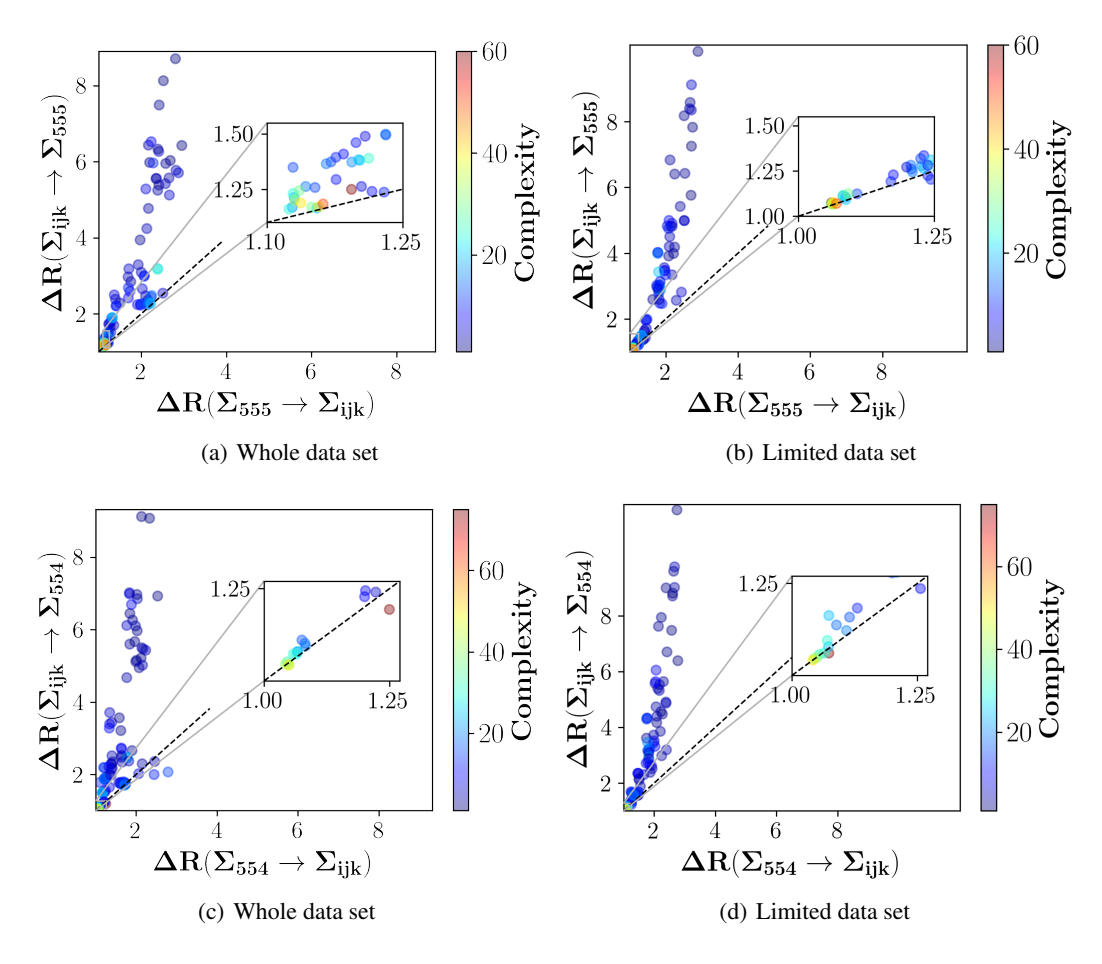


Figure D.3: Correlation plot between rank information imbalances of inferring all other descriptors from (a,b) Σ_{555} , (c,d) Σ_{554} (on x-axis) and inferring (a,b) Σ_{555} , (c,d) Σ_{554} from all other descriptors (on y-axis) for (a,c) the whole and (b,d) limited data sets.

E APPENDIX: A LINEAR MODEL FOR FORMATION ENERGY PREDICTIONS

We also fitted a linear model to the entirety of the limited data set (the training set contains the entirety of the limited data set). The relative ordering of descriptors from Figures [C.1], [D.1] and [E.1] is slightly different. Note that with the information-theoretic approach, we aim to construct a universal GSD instead of one only useful for the formation energy prediction task. So similar model analyses for other properties are also needed before choosing the universal optimally compressed global descriptor.

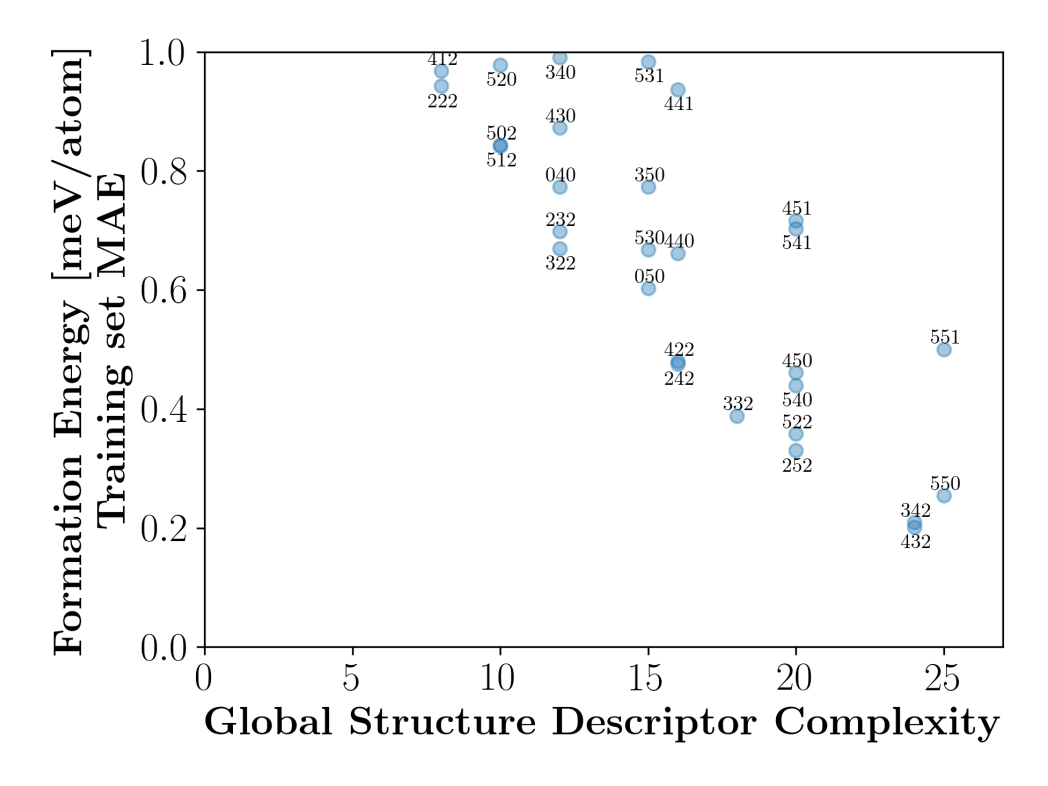


Figure E.1: MAE score of a simple linear regression model trained on the entirety of the limited data set as a function of descriptor complexity. Note that only a small number of relevant descriptors are depicted.